Title

Cell Migration and Bone Formation from Mesenchymal Stem Cell Spheroids in Alginate Hydrogels Are Regulated by Adhesive Ligand Density

Journal

Biomacromolecules, 18(12)

ISSN

1525-7797

Authors

Ho, Steve S
Keown, Andrew T
Addison, Bennett
et al.

Publication Date

2017-12-11

DOI

10.1021/acs.biomac.7b01366

Peer reviewed

HHS Public Access

Author manuscript

Biomacromolecules. Author manuscript; available in PMC 2018 December 11.

Published in final edited form as:

Biomacromolecules. 2017 December 11; 18(12): 4331–4340. doi:10.1021/acs.biomac.7b01366.

Cell Migration and Bone Formation from Mesenchymal Stem Cell Spheroids in Alginate Hydrogels Are Regulated by Adhesive Ligand Density

Steve S. Ho[†], **Andrew T. Keown**[†], **Bennett Addison**[†], and **J. Kent Leach**[†,‡,*,iD]

[†]Department of Biomedical Engineering, University of California, Davis, Davis California 95616, United States

[‡]Department of Orthopaedic Surgery, UC Davis Health, Sacramento California 95817, United States

Abstract

The adhesion and migration of cells entrapped in engineered materials is regulated by available adhesive ligands. Although mesenchymal stem cell (MSC) spheroids injected into damaged tissues promote repair, their transplantation in biomaterials which regulate cell migration from the aggregate may further enhance their therapeutic potential. Alginate hydrogels were modified with Arginine-Glycine-Aspartic acid (RGD) at increasing concentrations, and osteogenically induced human MSC spheroids were entrapped to assess cell migration, survival, and differentiation. Cell migration was greater from MSC spheroids in alginate modified with low RGD levels, while the osteogenic potential was higher for spheroids entrapped in unmodified or high RGD density gels *in vitro*. Upon ectopic implantation, microCT and immunohistochemistry revealed extensive osteogenesis in unmodified and high RGD density gels compared to low RGD density gels. These data suggest that restriction of MSC migration from spheroids correlates with enhanced spheroid osteogenic potential, representing a novel tool for bone tissue engineering.

Graphical abstract

[*]**Corresponding Author:** jkleach@ucdavis.edu.

ORCID

J. Kent Leach: 0000-0002-1673-3335

ASSOCIATED CONTENT

Supporting Information

The Supporting Information is available free of charge on the ACS Publications website at DOI: 10.1021/acs.biomac.7b01366.

Video 1: Time lapse video of cell migration from MSC spheroids in DS2 alginate over 7 days (AVI)

Video 2: Time lapse video of cell migration from MSC spheroids in DS10 alginate over 7 days (AVI)

Video 3: Time lapse video of cell migration from MSC spheroids in unmodified (UM) alginate over 7 days (AVI)

Author Contributions

The manuscript was written through contributions of all authors.

All authors have given approval to the final version of the manuscript.

Notes

The authors declare no competing financial interest.

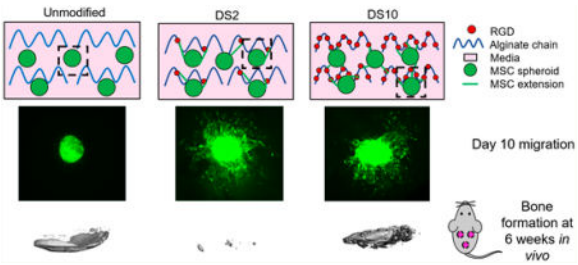

INTRODUCTION

When used in cell-based tissue regeneration, mesenchymal stem cells (MSCs) are often implanted directly into a defect site and perish within a few days, thus severely hindering their efficacy in promoting tissue repair.[1] Injected MSCs adhere and spread on native extracellular matrix (ECM) such as bone endosteum, and do not naturally exist as spheroids *in vivo*.[2] Yet, the therapeutic benefits of MSCs can be enhanced by forming them into 3-dimensional spheroids *in vitro* prior to implantation. Compared to individual cells, MSC spheroids demonstrate increased anti-apoptotic, pro-angiogenic, anti-inflammatory, and osteogenic potential,[3–6] suggesting that spheroids are a promising option for enhancing the efficacy of cell-based therapies.

The transplantation of osteogenically induced MSCs improves bone formation compared to undifferentiated cells, as induced MSCs may directly participate in osteogenesis.[7,8] Despite effective means to osteogenically induce MSCs in culture, cells rapidly dedifferentiate *in vitro* or *in vivo* upon removal of osteoinductive stimuli, thereby limiting their potential to promote bone repair.[9] Harvesting MSCs from the culture dish separates them from their endogenous ECM, representing a possible cause for reduced cell viability upon transplantation.[10] Culture of MSCs in osteoinductive media increases the deposition of key matricellular proteins such as collagen and fibronectin, which drives MSC adhesion and osteogenic differentiation following engagement of integrins with the ECM.[11] Unlike conventional cultures, MSC spheroids retain their endogenous ECM, which enhances the persistence of the osteoblastic phenotype compared to individual cells in the absence of soluble osteoinductive cues.[6] ECM retention may prevent cell death upon transplantation, further enhancing the survival and function of MSC spheroids.

Whereas others have injected spheroids *in vivo* without a biomaterial carrier, [4] primarily for promoting neovascularization of ischemic tissue, such an approach allows MSC migration from the spheroid to be instructed by the native, and potentially damaged, tissue ECM. As an alternative, entrapment of MSC spheroids within engineered materials can localize cells at the defect site, regulate migration of cells from the spheroids to the surrounding tissue, and modulate spheroid function. MSC response to engineered materials can be influenced by many properties including bulk substrate stiffness, degradation, and the identity and concentration of adhesive ligands presented to the cells. [12,13] We previously demonstrated that MSC pro-angiogenic potential and survival were enhanced when MSC spheroids were entrapped in alginate hydrogels presenting integrin-binding Arg-Gly-Asp (RGD) peptides to facilitate adhesion and migration.[5] Rapid cellular migration from the spheroid may translate

to MSC behavior characteristic of individual cells, thus limiting the benefit attained by spheroidal culture. As maintenance of spheroidal morphology may be important for sustained therapeutic potential, the relationship between cell adhesion, cell migration, and RGD concentration is a critical aspect for consideration when transplanting MSC spheroids.[14,15]

The hypothesis of this study was twofold: (1) osteoinduction under spheroidal culture will improve maintenance of osteogenic phenotype compared to MSCs induced in monolayer culture; and (2) RGD ligand density in alginate hydrogels regulates cell migration from entrapped spheroids and subsequent therapeutic potential. To test these hypotheses, we entrapped osteoinduced MSC spheroids in alginate hydrogels with increasing levels of RGD conjugation and characterized the effect on cell migration, osteogenic potential, and the capacity to promote bone formation *in vivo*.

MATERIALS AND METHODS

Cell Culture and Spheroid Formation

Human bone marrow-derived MSCs from a single donor were purchased from Lonza (Walkersville, MD) and used without further characterization. Cells were cultured in α-MEM (Invitrogen, Carlsbad, CA) supplemented with 10% fetal bovine serum (JR Scientific, Woodland, CA), 100 units/mL penicillin, and 100 μg/mL streptomycin (Gemini Bio Products, Woodland, CA) under standard culture conditions until use at passage 5–6.

MSCs were osteogenically induced either in monolayer or as spheroids. For monolayer induction, MSCs were seeded at 5,000 cells/cm^2 in culture flasks and maintained in osteogenic media (growth media containing the standard osteogenic supplements of 10 mM β-glycerophosphate, 50 μg/mL ascorbate-2-phosphate, and 100 nM dexamethasone; all from Sigma-Aldrich, St. Louis, MO) for 12 days. MSCs were then trypsinized and formed into spheroids of 15,000 MSCs in osteogenic media using a forced aggregation technique.[16] Plates were kept static in a standard incubator for 48 h to allow for spheroid compaction. For induction as spheroids, MSCs were first formed into spheroids in osteogenic media and transferred to 6-well plates containing 2 mL of 1.5% agarose to prevent adhesion to tissue culture plastic (TCP). Spheroids were maintained in osteogenic media for an additional 12 days, resulting in a total osteoinduction period of 14 days for both conditions.

Preparation of RGD-Modified Alginate and Entrapment of MSC Spheroids

RGD-modified alginate was prepared as described previously.[5,17,18] Briefly, G_4RGDSP (Commonwealth Biotechnologies, Richmond, VA) was covalently coupled to UltraPure VLVG sodium alginate (Pronova, Lysaker, Norway) using standard carbodiimide chemistry, yielding hydrogels with a degree of substitution (DS) of DS0.5, DS2, DS5, and DS10. Degree of substitution is defined as the number of peptide ligands conjugated to a single alginate polymer chain. These values correspond to bulk RGD densities of 0.2, 0.8, 2, and 4 mM, respectively. The resulting RGD-alginate was sterile filtered and lyophilized for 4 days. Lyophilized alginate was reconstituted in serum-free α-MEM to obtain a 2.1% (w/v)

solution. MSC spheroids were then entrapped in alginate and cross-linked by exposure to 200 mM $CaCl_2$ for 10 min as described.[5]

Confirmation of RGD Conjugation via ^{1}H NMR

All NMR data were collected at 25 °C on an 800 MHz Bruker Avance III NMR spectrometer equipped with a 5 mm CPTCI H/C/N/D Z-gradient cryogenic probe with standard gradient coils capable of 50 G/cm gradient pulses. Chemical shifts were referenced to the residual water peak at 4.7 ppm. Routine ^{1}H NMR spectra were collected using a 30° tip angle, 64 scan averages, 3 s acquisition time, and a 3 s recycle delay. ^{1}H DOSY/Diffusion NMR acquisition parameters were: dstebpgp3s Bruker pulse program, 8 scans and 16 DOSY points, 7 ppm spectral width, 3 s acquisition time, and a 3 s recycle delay. The diffusion delays “big-delta” and “little-delta” were set to 100 and 2 ms, respectively. Data were processed using DosyToolbox version 2.5. Each individual FID was phased and baseline corrected, and the decaying peak heights were fit by DosyToolbox.

Assessment of Hydrogel Mechanical Properties

The viscoelastic properties of alginate gels were measured using a Discovery HR2 Hybrid Rheometer (TA Instruments, New Castle, DE). An 8.0-mm-diameter Peltier plate geometry was used for 80 μL gels with corresponding 8.0 mm diameter. Gels were cross-linked and then maintained in media under standard culture conditions for 24 h before measurement. An oscillatory strain sweep ranging from 0.004% to 4% strain was performed on each gel to obtain the linear viscoelastic region (LVR) before gel failure. At least 10 data points were collected for the LVR and averaged to obtain gel shear storage modulus.

Analysis of MSC Spheroid Function within Alginate Gels

MSCs were entrapped in alginate gels at 5×10^6 cells/mL. To determine MSC vulnerability to apoptosis, gels were cultured in α-MEM under serum-deprived and hypoxic (1% O_2) culture conditions for 4 days, minced, and lysed in passive lysis buffer (Promega, Madison, WI). We previously observed apoptosis in MSCs under these conditions, and apoptosis was quantitatively measured by analyzing 100 μL lysate per sample using a Caspase-Glo 3/7 assay (Promega).[19] Luminescence was detected on a microplate reader and normalized to DNA content determined from the same lysate using the Quant-iT PicoGreen DNA Assay Kit (Invitrogen). In order to measure VEGF secretion, media was refreshed 24 h before collection, and VEGF concentration was determined using a human specific VEGF ELISA kit (R&D Systems, Minneapolis, MN) according to the manufacturer’s instructions.[20]

To quantify maintenance of osteogenic potential of entrapped spheroids, gels containing osteoinduced MSC spheroids were cultured in α-MEM lacking osteoinductive cues for 7 days under standard culture conditions. Osteogenic potential was assessed by quantifying intracellular alkaline phosphatase (ALP) activity from a p-nitrophenyl phosphate assay, osteocalcin secretion via ELISA (R&D Systems), and calcium deposition by *o*-cresolphthalein assay. [17,21,22]

Evaluation of Cell Migration from Spheroids via Time Lapse Microscopy

GFP-expressing human MSCs (UC Davis Institute for Regenerative Cures, Davis, CA) were culture expanded and osteoinduced as spheroids for 14 days. Spheroids were entrapped in RGD-modified alginate hydrogels with varying ligand densities. The hydrogel was placed directly into the bottom of a nonadherent 48 well plate and cultured in growth media for the remainder of the study. Fluorescent images were taken for 12–15 time points a day for 7 days to create time-lapse videos. Images were processed using NIH ImageJ software. Distance of MSC migration and number of extensions from the spheroids were quantified using NIS-Elements software.

In Vivo Subcutaneous Implantation

Treatment of all experimental animals was in accordance with UC Davis animal care guidelines and all National Institutes of Health animal handling protocols. Eight-week-old non-obese diabetic/severe combined immunodeficient gamma (NSG, NOD.Cg-Prkdc^{scid} Il2rg^{tm1Wjl}/ SzJ) mice (Jackson Laboratories) were anesthetized and maintained under a 2% isoflurane/O_2 mixture delivered through a nose cone. Osteoinduced spheroids were entrapped in alginate hydrogels (80 μL) at 30 × 10^6 cells/mL as described above. Two longitudinal incisions were made in the dorsum, and subcutaneous pockets were created on each side of the incision for biomaterial implantation, after which surgical sites were closed with staples. Animals were euthanized after 2 and 6 weeks by CO_2 inhalation. Alginate gels were explanted, fixed in phosphate buffered formalin for 24 h, and maintained in 70% ethanol until analysis.

Quantification of Neovascularization and Bone Formation

Two weeks post-implantation, constructs were processed, paraffin-embedded, and sectioned at 5 μm. Sections were stained with hematoxylin and eosin (H&E) and imaged using a Nikon Eclipse TE2000U microscope and Andor Zyla 5.5 sCMOS digital camera (Concord, MA). Blood vessel formation was quantified using NIS-Elements software. In order to visualize transplanted human cells, sections underwent immunohistochemistry (IHC) using a primary antibody against lamin A/C (1:250, ab108595, Abcam), a human nuclear envelope marker.

At 6 weeks post-implantation, all remaining animals were euthanized and gels were explanted, fixed in 10% formalin for 24 h, and transferred to 70% ethanol. Constructs were imaged (45 kVp, 177 μA, 400 μs integration time, average of four images) at 6 μm resolution using a high-resolution μCT specimen scanner (μCT 35; Scanco Medical, Brüttisellen, Switzerland). Bone volume fraction (BVF) and bone mineral density (BMD) were determined from resulting images using the accompanying software. Explants were then demineralized in Calci-Clear Rapid (National Diagnostics, Atlanta, GA), processed, paraffin-embedded, and sectioned at 5 μm thickness. Sections were stained with H&E and Masson's Trichrome. To visualize cells undergoing osteogenic differentiation, we performed IHC on sections using a primary antibody against osteocalcin (1:1000, ab13420, Abcam) and a mouse specific HRP/AEC detection kit (ab93705, Abcam).

Statistical Analysis

Data are presented as means and standard deviation. Statistical analysis was performed using a two-way analysis of variance with Bonferroni correction for multiple comparisons in Prism 6 software (GraphPad, San Diego, CA); *p*-values less than 0.05 were considered statistically significant. Significance is denoted by alphabetical letterings; groups with no significance are linked by the same letters, while groups with significance do not share the same letters.

RESULTS

RGD Conjugation to Alginate and Mechanical Characterization

We used single proton nuclear magnetic resonance (^{1}H NMR) to confirm differences in RGD incorporation onto the alginate. From the spectra, we detected proton peaks indicative of arginine (Figure 1A). No identifiable peaks were seen in the unmodified or DS0.5 groups. The magnitude of proton peaks correlated with the degree of RGD substitution for DS2, DS5, and DS10 alginates (2, 5.8, and 10, respectively). Diffusion ordered spectroscopy (DOSY) revealed diffusive properties of small molecules in the sample. RGD peptide peaks corresponded to lower diffusion coefficients at the same level as alginate polymer, indicating stable ligand conjugation (Figure 1B). Higher diffusion coefficients were detected that were attributed to the free-floating unconjugated EDC cross-linker.

We tested mechanical properties of acellular alginate hydrogels at all degrees of substitution via rheology (Figure 1C). No differences in storage moduli were detected, regardless of RGD conjugation.

Osteoinduction of MSCs in Spheroid Culture Improves Cell Viability and Osteogenesis

Caspase activity increased from Day 1 to Day 4 in all gels containing MSCs osteoinduced in monolayer, and RGD ligand density did not affect caspase activity in MSC spheroids (Figure 2A). Conversely, MSCs osteoinduced as spheroids and entrapped in RGD-modified alginate exhibited reduced caspase activity compared to spheroids in unmodified alginate at both time points (Figure 2B). Caspase activity decreased from Day 1 to Day 4 among RGD-conjugated groups only.

We evaluated osteogenic differentiation of spheroids that were osteoinduced in monolayer prior to spheroid formation (Figure 2C, E, G) or as spheroids (Figure 2D, F, H). ALP activity of monolayer induced MSC spheroids was similar in all groups over 7 days, regardless of RGD ligand density (Figure 2C). No detectable calcium deposition was observed in any gel over 7 days (Figure 2E). At Day 7, osteocalcin secretion was highest from spheroids in unmodified alginate and decreased with increasing ligand density (Figure 2G). In MSCs osteoinduced as spheroids, ALP activity was highest in unmodified alginate and decreased with RGD conjugation (Figure 2D). Calcium deposition was greatest when osteoinduced spheroids were entrapped in unmodified gels (Figure 2F). At Day 4, calcium deposition increased with ligand density, yet this trend was less apparent at 7 days. Similar to ALP and calcium, osteocalcin secretion by osteoinduced MSC spheroids was highest, on average, in unmodified alginate at Day 4 (Figure 2H). No differences were observed among ligand

densities at Day 7. Overall, expression of these three osteoblastic markers (ALP activity, calcium deposition, and osteocalcin secretion) was greater when MSCs were induced as spheroids than under monolayer culture. Minimal differences in osteogenic differentiation were detected for spheroids entrapped in DS5 and DS10 hydrogels. Therefore, ensuing osteoinduction was performed under spheroid culture and studied in unmodified, DS2, or DS10 RGD-modified alginate gels.

Proangiogenic Potential and MSC Proliferation Is Increased with RGD Density

We assessed the proangiogenic potential of MSCs osteoinduced as spheroids by quantifying secreted VEGF (Figure 3). Osteoinduced MSC spheroids secreted the most total VEGF when entrapped in DS10 alginate (Figure 3A). DNA quantification revealed higher DNA content in DS10 gels at Day 1 compared to other groups, but no differences at Day 4 (Figure 3B).

Increased RGD Density Slows MSC Migration and Enhances Adhesion

We assessed migration of MSCs from osteoinduced spheroids during culture in growth media over 10 days (Figure 4). At 6 days, MSCs in DS2 alginate had migrated farther than MSCs in DS10 alginate (Figure 4A, Video S1 and S2, respectively). This difference became more apparent after 10 days. MSCs in unmodified alginate did not adhere or spread in the hydrogel (Video S3). Differences in the number of extensions from the spheroids were evident at early time points (Figure 4B). Spheroids in DS10 alginates exhibited greater cell sprouting than spheroids in DS2 alginate at Day 4 and beyond. In agreement with migration, MSCs in unmodified alginate demonstrated no evident cell sprouting from osteoinduced spheroids. Finally, we quantified the change in total area covered by MSCs over 7 days, which revealed greater coverage from spheroids in DS2 gels compared to DS10 gels (Figure 4C). Fluorescent images of spheroids at Day 10 indicate no migration in unmodified alginate gels, long and scattered migration in DS2 gels, and short and dense sprouting from MSC spheroids in DS10 gels (Figure 4D).

MSC Spheroids Transplanted in RGD-Modified Alginate Enhance Angiogenesis In Vivo

H&E staining of 2-week explants revealed extensive host cell ingrowth in all RGD-modified alginate groups (Figure 5A), while host cell infiltration was not apparent in unmodified alginate gels. Lamin A/C staining indicated the presence of human MSCs in all explants. MSC spheroids in DS2 and DS10 alginate exhibited more clustered staining than those in unmodified alginate. We detected greater blood vessel density in all RGD-modified groups compared to spheroids in unmodified alginate (Figure 5B). However, no differences in neovascularization were associated with ligand density.

Bone Formation Is Enhanced with Osteoinduced Spheroids by Restricting Cell Migration

MicroCT imaging revealed more mineralized tissue when osteoinduced MSC spheroids were implanted in unmodified alginate gels or DS10 alginate groups compared to DS2 alginate (Figure 6A). Lateral μCT images revealed clear localization of mineral on a single plane with spheroids in unmodified gels. However, bone formation was more distributed throughout the gel structure from spheroids transplanted in DS10 alginate. Quantification of

bone volume and bone mineral density correlated with microCT scans (Figure 6B, C). H&E staining revealed minimal cell infiltration in unmodified alginate gels, while RGD-modified gels were more cellularized (Figure 6D). The volume of DS2 alginate gels was appreciably smaller than all other groups. Masson's trichrome staining revealed collagen deposition on the exterior of all gels. In all RGD-containing alginate gels, extensive collagen deposition was visible throughout the gel, especially in the DS10 alginate. Immunohistochemistry for osteocalcin demonstrated diffuse staining throughout the unmodified alginate gel and darker staining in encapsulating tissue. Osteocalcin staining in RGD-modified alginate gels revealed apparent, localized areas of staining.

DISCUSSION

The entrapment of cells in engineered materials facilitates the instruction of cell function when used for tissue regeneration. MSCs used for bone tissue engineering commonly undergo osteoinduction with biochemical supplements to generate cells that can mineralize directly upon transplantation *in vivo*.[23,24] Naïve MSC spheroids transplanted in RGD-modified alginate form bone in an ectopic site.[5] However, constructs transplanted into critical sized femoral defects did not sufficiently mineralize, even with codelivery of 1.5 μg of bone morphogenetic protein-2 (BMP-2).[25] RGD concentration was not reported, and supraphysiological doses of BMP-2 are associated with numerous complications and high cost.[26] Osteoinduced spheroids retain their osteoblastic markers better than individual MSCs,[6] further motivating the transplantation of MSC spheroids for bone tissue engineering. Herein, we investigated the interplay between RGD ligand density on alginate gels and cell migration from osteoinduced MSC spheroids on their capacity to form mineralized tissue *in vitro* and *in vivo*.

RGD peptide was successfully conjugated to alginate at increasing degrees of substitution. Furthermore, ligand densities did not affect storage modulus, eliminating concerns of variable bulk stiffness contributing to MSC response to the hydrogel.[27] By decoupling mechanical stiffness as a confounding factor in regulating cell adhesion and differentiation, we can attribute observed cellular responses to changes in RGD ligand density on the backbone of alginate hydrogels. We observed arginine peaks with ^{1}H NMR that increase in peak height with greater degree of substitution. The mass ratios were maintained, confirming precise differences in conjugation. RGD diffusional coefficients were low, indicating stable conjugation to the alginate polymer.

We evaluated the survival and osteogenic potential of MSC spheroids osteoinduced in monolayer culture prior to spheroid formation or after MSCs were aggregated into spheroids. Quantification of osteogenic potential was determined in the absence of osteoinductive cues to model cell response upon transplantation. Caspase 3/7 activity, an indicator of apoptosis, was decreased in spheroid-induced MSCs in accordance with previous studies demonstrating reduced caspase activity in spheroids versus individual cells.[5,20] In addition, endogenous matrix production can contribute to enhanced viability in spheroid-induced MSCs.[28] Monolayer-induced spheroids do not retain ECM deposited during the osteoinduction period. However, spheroid-induced MSCs continuously secrete and mineralize an endogenous matrix that is maintained after entrapment in alginate, thus

improving osteogenic potential. Cell viability may also be dependent upon differentiation state, as osteogenically induced MSCs exhibit improved survival over undifferentiated cells.[9,19] Indeed, *RUNX2* expression, a key osteogenic transcription factor, can activate phosphotidyl inositol 3′ kinase (PI3K) signaling pathways that promote cell survival.[29] These data demonstrate that osteoinduction of MSCs as spheroids is more effective to enhance MSC viability and osteogenic potential.

We investigated the balance between osteogenic differentiation and cell migration in osteoinduced spheroids by entrapping them in RGD-modified alginate. MSCs at later stages of osteogenic differentiation exhibit slower migration but greater adhesivity, further motivating the need for understanding the link between migration of cells from spheroids and material properties.[30] In these studies, we observed the natural tendency of cells to attach and migrate when engaging RGD ligands instead of remaining attached to endogenous ECM proteins containing similar adhesion sites. The fraction of actively migrating cells represents a small percentage of the overall cell density in the gels and would behave like an individual cell, potentially reducing the overall therapeutic potential of an intact spheroid with few migrating cells. Assuming uniform spherical shape and a radius of 200 μm, only 1.5% of the MSCs initially engage RGD, a number which increases with migration over time. MSC migration was more rapid from spheroids entrapped in low RGD alginate compared to high RGD alginate. However, spheroid morphologies were visibly different in these two gels, with greater cellular adhesion in DS10 alginate. This behavior can be attributed to the higher density of adhesion sites available for binding. In hyaluronic acid hydrogels, murine MSCs migrated faster in gels with 1 mM bulk RGD density compared to 0.1 mM RGD.[14] Our results demonstrate that a bulk density of 4 mM RGD (DS10) slows cell spreading compared to 0.8 mM (DS2) RGD alginate gels, suggesting there is an optimal RGD density in alginate gels with these mechanical properties to enhance cell migration. Additionally, ascorbic acid within the osteoinductive cocktail stimulates matrix production,[31] which is retained in spheroids and not lost upon trypsinization. Upon entrapment in alginate, MSCs are exposed to covalently linked RGD ligands presented in a controlled manner, while the intraspheroidal ECM contains matrix proteins that engage many cell surface integrins, primarily of the β1 family.[32] Further investigation is needed to understand how migration and phenotype of MSCs in spheroids is affected by the identity and concentration of matricellular proteins and peptides.

The density of RGD on the backbone of polymeric hydrogels has a profound effect on MSC therapeutic potential,[33–35] but the effect of this stimulus has not previously been investigated in MSC spheroids through modulation of cell migration. MSC spheroids in DS10 alginate secreted the most VEGF, likely a function of increased cell number. These data suggest that impaired migration kinetics could regulate angiogenic potential of osteoinduced spheroids. DS10 alginate may act as a “cage” for MSC spheroids, slowing initial migration due to an abundance of adhesion sites. Adhesion and angiogenesis is linked through Hypoxia Inducible Factor −1α (HIF-1α), a master transcription factor regulating cell viability and angiogenesis. In glioblastoma aggregate culture, HIF-1α is mediated through highly expressed αvβ3/αvβ5 integrins, resulting in activation of focal adhesion kinase (FAK),[36] but this has not been demonstrated in MSCs. Increased migration of cells from spheroids in DS2 alginates could decrease HIF-1α expression through attenuated engagement of αvβ3/αvβ5

integrins and decreased formation of focal adhesions,[33] in turn mitigating VEGF secretion.[37] Our *in vitro* data confirm increased osteogenesis when osteoinduced MSC spheroids were entrapped in unmodified and DS10 alginate compared to DS2 alginate. RGD spacing may also represent a key underlying contributor. MSCs and MC3T3 cells in RGD alginate gels had increasing osteogenic potential with decreased RGD ligand spacing,[38,39] which is in agreement with our high RGD alginate presenting shorter ligand spacing. MSC spheroids in DS10 alginate could form focal adhesions that regulate cell spreading and differentiation.[38] Increased integrin clustering in high density RGD microenvironments upregulates cytoskeletal tension and activates the ERK1/2 pathway to initiate osteogenic differentiation.[40] This could explain how osteogenesis decreases in spheroids in DS2 alginate as cells migrate outward yet increases in DS10 alginate. Together, these data demonstrate a complex relationship between MSC adhesion and spheroid viability, VEGF secretion, and osteogenesis.

Finally, we encapsulated spheroids in alginate hydrogels of low and high RGD density to ascertain potential differences in bone formation. Overall, we observed the most bone formation when implanting osteoinduced spheroids in unmodified alginate. Between RGD-modified gels, MSC spheroids transplanted in DS10 alginate resulted in higher bone volume, on average, than DS2 alginate ($p = 0.0554$). H&E staining of unmodified gel explants demonstrated minimal host cell infiltration, and μCT revealed mineral localization to the hydrogel exterior. This could be the result of spheroid calcium secretion that binds to the surrounding fibrous tissue, as unmodified alginate does not support cell adhesion and matrix deposition due to its nonfouling nature. Bone formation likely occurs following degradation of the alginate and invasion of host cells into the tissue site. Compared to the other implants, we detected less residual alginate in the DS2 hydrogels, as well as minimal bone formation, which could indicate accelerated host cell infiltration and degradation of the hydrogel. We previously demonstrated strong mineralization from naïve MSC spheroids in 0.32 mM bulk density RGD alginate gels *in vivo*.[5] However, that study utilized a higher cell density (40×10^6 cells/mL), a different cell and biomaterial source, and proceeded for 8 weeks, allowing for more mature tissue to form. Here, spheroids in DS10 alginate resulted in strong bone formation and matrix deposition as indicated by μCT and histology. These data indicate that DS10 alginate can facilitate bone formation with osteoinduced spheroids in an ectopic site even after 6 weeks. This work provides further insight into the importance of spheroid osteoinduction prior to transplantation and that appropriate presentation of adhesion ligands can maintain osteogenic potential of entrapped spheroids.

CONCLUSIONS

These studies demonstrate that RGD peptide density in alginate hydrogels regulates adhesion and migration kinetics of cells from osteoinduced MSC spheroids. Corresponding adhesion or lack of adhesion can each drive osteogenesis of entrapped cells. Furthermore, osteoinduction in spheroidal culture enhances osteogenic potential of MSCs compared to spheroids formed from cells osteogenically induced in monolayer culture. Osteoinduction of MSC spheroids and their subsequent delivery in highly substituted RGD alginate gels should be considered for their ability to drive both angiogenesis and bone formation.

Supplementary Material

Refer to Web version on PubMed Central for supplementary material.

Acknowledgments

This work was supported by the National Institutes of Health (R01 DE025475) to J.K.L. S.H. was supported by the T32 Animal Models of Infectious Disease Training Program Kirschstein-NRSA (T32 AI060555). The content is solely the responsibility of the authors and does not necessarily represent the official views of the National Institutes of Health. The funders had no role in the decision to publish or preparation of the manuscript. The authors acknowledge Tanya Garcia-Nolan for assistance in obtaining microCT data.

References

1. McGinley LM, McMahon J, Stocca A, Duffy A, Flynn A, O'Toole D, O'Brien T. Mesenchymal stem cell survival in the infarcted heart is enhanced by lentivirus vector-mediated heat shock protein 27 expression. Hum. Gene Ther. 2013; 24(10):840–51. [PubMed: 23987185]
2. Ehninger A, Trumpp A. The bone marrow stem cell niche grows up: mesenchymal stem cells and macrophages move in. J. Exp. Med. 2011; 208(3):421–8. [PubMed: 21402747]
3. Bartosh TJ, Ylostalo JH, Mohammadipoor A, Bazhanov N, Coble K, Claypool K, Lee RH, Choi H, Prockop DJ. Aggregation of human mesenchymal stromal cells (MSCs) into 3D spheroids enhances their antiinflammatory properties. Proc. Natl. Acad. Sci. U. S.A. 2010; 107(31):13724–9. [PubMed: 20643923]
4. Bhang SH, Lee S, Shin JY, Lee TJ, Kim BS. Transplantation of cord blood mesenchymal stem cells as spheroids enhances vascularization. Tissue Eng., Part A. 2012; 18(19–20):2138–47. [PubMed: 22559333]
5. Ho SS, Murphy KC, Binder BY, Vissers CB, Leach JK. Increased survival and function of mesenchymal stem cell spheroids entrapped in instructive alginate hydrogels. Stem Cells Transl. Med. 2016; 5(6):773–81. [PubMed: 27057004]
6. Murphy KC, Hoch AI, Harvestine JN, Zhou D, Leach JK. Mesenchymal stem cell spheroids retain osteogenic phenotype through alpha2beta1 signaling. Stem Cells Transl. Med. 2016; 5(9):1229–37. [PubMed: 27365484]
7. Shin M, Yoshimoto H, Vacanti JP. In vivo bone tissue engineering using mesenchymal stem cells on a novel electrospun nanofibrous scaffold. Tissue Eng. 2004; 10(1–2):33–41. [PubMed: 15009928]
8. Castano-Izquierdo H, Alvarez-Barreto J, van den Dolder J, Jansen JA, Mkos AG, Sikavitsas VI. Pre-culture period of mesenchymal stem cells in osteogenic media influences their in vivo bone forming potential. J. Biomed. Mater. Res., Part A. 2007; 82(1):129–38.
9. Hoch AI, Mittal V, Mitra D, Vollmer N, Zikry CA, Leach JK. Cell-secreted matrices perpetuate the bone-forming phenotype of differentiated mesenchymal stem cells. Biomaterials. 2016; 74:178–87. [PubMed: 26457835]
10. Harvestine JN, Vollmer NL, Ho SS, Zikry CA, Lee MA, Leach JK. Extracellular matrix-coated composite scaffolds promote mesenchymal stem cell persistence and osteogenesis. Biomacromolecules. 2016; 17(11):3524–3531. [PubMed: 27744699]
11. Kundu AK, Putnam AJ. Vitronectin and collagen I differentially regulate osteogenesis in mesenchymal stem cells. Biochem. Biophys. Res. Commun. 2006; 347(1):347–57. [PubMed: 16815299]
12. Leach JK, Whitehead J. Materials-directed differentiation of mesenchymal stem cells for tissue engineering and regeneration. ACS Biomater. Sci. Eng. 2017; doi: 10.1021/acsbiomaterials.6b00741
13. Lutolf MP, Gilbert PM, Blau HM. Designing materials to direct stem-cell fate. Nature. 2009; 462(7272):433–41. [PubMed: 19940913]
14. Lei Y, Gojgini S, Lam J, Segura T. The spreading, migration and proliferation of mouse mesenchymal stem cells cultured inside hyaluronic acid hydrogels. Biomaterials. 2011; 32(1):39–47. [PubMed: 20933268]

15. Rowley JA, Mooney DJ. Alginate type and RGD density control myoblast phenotype. J. Biomed. Mater. Res. 2002; 60(2):217–23. [PubMed: 11857427]
16. Dahlmann J, Kensah G, Kempf H, Skvorc D, Gawol A, Elliott DA, Drager G, Zweigerdt R, Martin U, Gruh I. The use of agarose microwells for scalable embryoid body formation and cardiac differentiation of human and murine pluripotent stem cells. Biomaterials. 2013; 34(10):2463–71. [PubMed: 23332176]
17. Bhat A, Hoch AI, Decaris ML, Leach JK. Alginate hydrogels containing cell-interactive beads for bone formation. FASEB J. 2013; 27(12):4844–52. [PubMed: 24005905]
18. Rowley JA, Madlambayan G, Mooney DJ. Alginate hydrogels as synthetic extracellular matrix materials. Biomaterials. 1999; 20(1):45–53. [PubMed: 9916770]
19. Binder BY, Genetos DC, Leach JK. Lysophosphatidic acid protects human mesenchymal stromal cells from differentiation-dependent vulnerability to apoptosis. Tissue Eng., Part A. 2014; 20(7–8): 1156–64. [PubMed: 24131310]
20. Murphy KC, Fang SY, Leach JK. Human mesenchymal stem cell spheroids in fibrin hydrogels exhibit improved cell survival and potential for bone healing. Cell Tissue Res. 2014; 357(1):91–9. [PubMed: 24781147]
21. Davis HE, Binder BY, Schaecher P, Yakoobinsky DD, Bhat A, Leach JK. Enhancing osteoconductivity of fibrin gels with apatite-coated polymer microspheres. Tissue Eng., Part A. 2013; 19(15–16):1773–82. [PubMed: 23560390]
22. Decaris ML, Binder BY, Soicher MA, Bhat A, Leach JK. Cell-derived matrix coatings for polymeric scaffolds. Tissue Eng., Part A. 2012; 18(19–20):2148–57. [PubMed: 22651377]
23. Dosier CR, Uhrig BA, Willett NJ, Krishnan L, Li MT, Stevens HY, Schwartz Z, Boyan BD, Guldberg RE. Effect of cell origin and timing of delivery for stem cell-based bone tissue engineering using biologically functionalized hydrogels. Tissue Eng., Part A. 2015; 21(1–2):156–65. [PubMed: 25010532]
24. Hoch AI, Binder BY, Genetos DC, Leach JK. Differentiation-dependent secretion of proangiogenic factors by mesenchymal stem cells. PLoS One. 2012; 7(4):e35579. [PubMed: 22536411]
25. Allen AB, Zimmermann JA, Burnsed OA, Yakubovich DC, Stevens HY, Gazit Z, McDevitt TC, Guldberg RE. Environmental manipulation to promote stem cell survival in vivo: use of aggregation, oxygen carrier, and BMP-2 co-delivery strategies. J. Mater. Chem. B. 2016; 4(20): 3594–3607.
26. Lissenberg-Thunnissen SN, de Gorter DJ, Sier CF, SchipperF IB. Use and efficacy of bone morphogenetic proteins in fracture healing. Int. Orthop. 2011; 35(9):1271–80. [PubMed: 21698428]
27. Pek YS, Wan AC, Ying JY. The effect of matrix stiffness on mesenchymal stem cell differentiation in a 3D thixotropic gel. Biomaterials. 2010; 31(3):385–91. [PubMed: 19811817]
28. Endres M, Hutmacher DW, Salgado AJ, Kaps C, Ringe J, Reis RL, Sittinger M, Brandwood A, Schantz JT. Osteogenic induction of human bone marrow-derived mesenchymal progenitor cells in novel synthetic polymer-hydrogel matrices. Tissue Eng. 2003; 9(4):689–702. [PubMed: 13678447]
29. Tandon M, Chen Z, Pratap J. Runx2 activates PI3K/Akt signaling via mTORC2 regulation in invasive breast cancer cells. Breast Cancer Res. 2014; 16(1):R16. [PubMed: 24479521]
30. Ichida M, Yui Y, Yoshioka K, Tanaka T, Wakamatsu T, Yoshikawa H, Itoh K. Changes in cell migration of mesenchymal cells during osteogenic differentiation. FEBS Lett. 2011; 585(24): 4018–24. [PubMed: 22100295]
31. Langenbach F, Handschel J. Effects of dexamethasone, ascorbic acid and beta-glycerophosphate on the osteogenic differentiation of stem cells in vitro. Stem Cell Res. Ther. 2013; 4(5):117. [PubMed: 24073831]
32. Docheva D, Popov C, Mutschler W, Schieker M. Human mesenchymal stem cells in contact with their environment: surface characteristics and the integrin system. J. Cell. Mol. Med. 2007; 11(1): 21–38. [PubMed: 17367499]
33. Kim IL, Khetan S, Baker BM, Chen CS, Burdick JA. Fibrous hyaluronic acid hydrogels that direct MSC chondrogenesis through mechanical and adhesive cues. Biomaterials. 2013; 34(22):5571–80. [PubMed: 23623322]

34. Yang F, Williams CG, Wang DA, Lee H, Manson PN, Elisseeff J. The effect of incorporating RGD adhesive peptide in polyethylene glycol diacrylate hydrogel on osteogenesis of bone marrow stromal cells. Biomaterials. 2005; 26(30):5991–8. [PubMed: 15878198]
35. Alsberg E, Anderson KW, Albeiruti A, Franceschi RT, Mooney DJ. Cell-interactive alginate hydrogels for bone tissue engineering. J. Dent. Res. 2001; 80(11):2025–9. [PubMed: 11759015]
36. Skuli N, Monferran S, Delmas C, Favre G, Bonnet J, Toulas C, Cohen-Jonathan Moyal E. Alphavbeta3/alphavbeta5 integrins-FAK-RhoB: a novel pathway for hypoxia regulation in glioblastoma. Cancer Res. 2009; 69(8):3308–16. [PubMed: 19351861]
37. Ruoslahti E. RGD and other recognition sequences for integrins. Annu. Rev. Cell Dev. Biol. 1996; 12:697–715. [PubMed: 8970741]
38. Comisar WA, Kazmers NH, Mooney DJ, Linderman JJ. Engineering RGD nanopatterned hydrogels to control preosteoblast behavior: a combined computational and experimental approach. Biomaterials. 2007; 28(30):4409–17. [PubMed: 17619056]
39. Frith JE, Mills RJ, Cooper-White JJ. Lateral spacing of adhesion peptides influences human mesenchymal stem cell behaviour. J. Cell Sci. 2012; 125:317–27. [PubMed: 22250203]
40. Biggs MJ, Dalby MJ. Focal adhesions in osteoneogenesis. Proc. Inst. Mech. Eng., Part H. 2010; 224(12):1441–53.

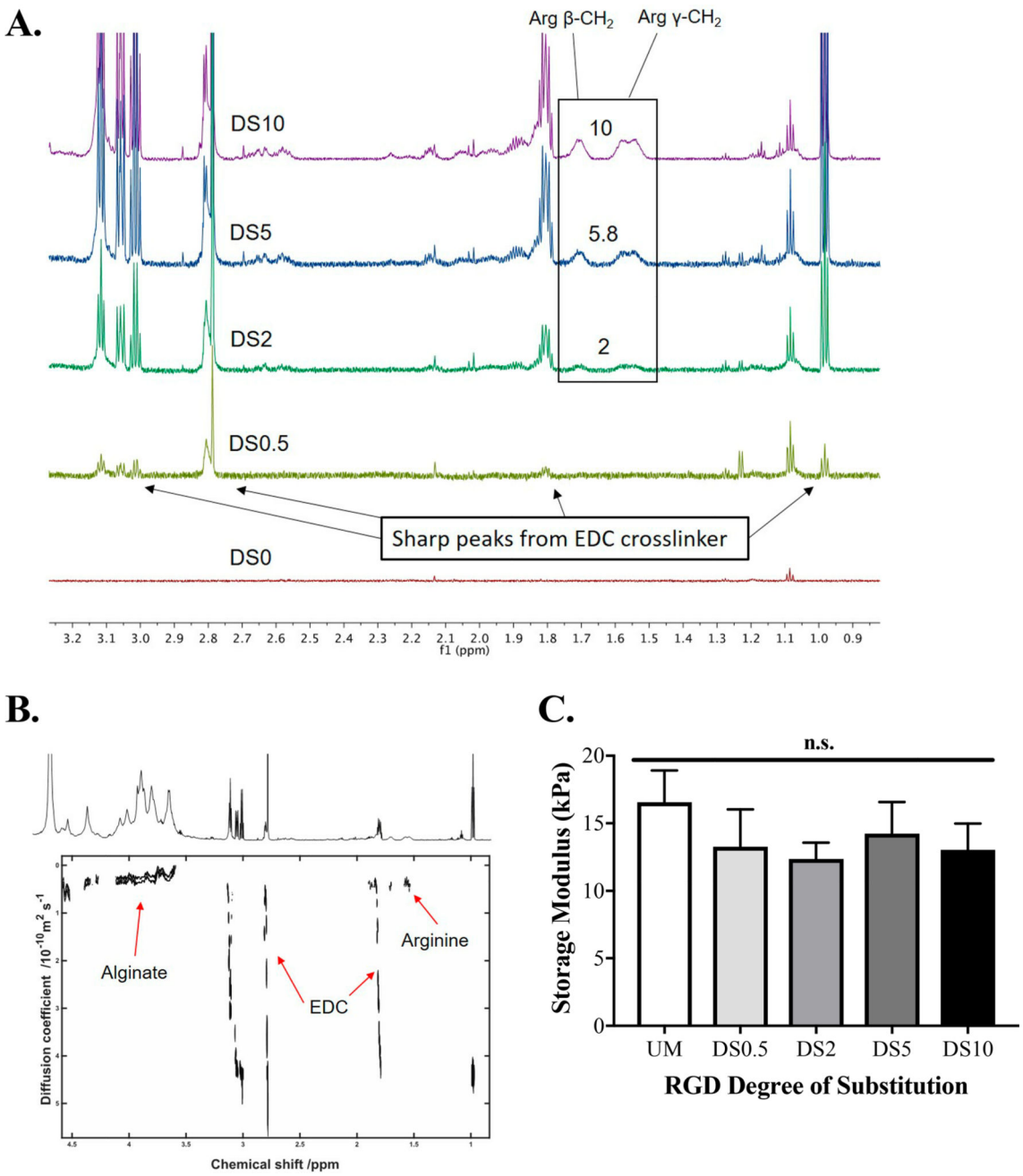

Figure 1.

Characterization of RGD-conjugation to alginate. (A) ^{1}H NMR spectra of all RGD ligand densities; DS0 (unmodified alginate), DS0.5, DS2, DS5, and DS10. (B) DOSY depicting diffusion coefficients of protons and corresponding effective conjugation of RGD to alginate backbone. Red arrows indicate protons that are indicative of either alginate, freely diffusing EDC, or peptide. (C) Storage modulus of all alginates; $n = 6$. UM = unmodified; n.s. = not significant.

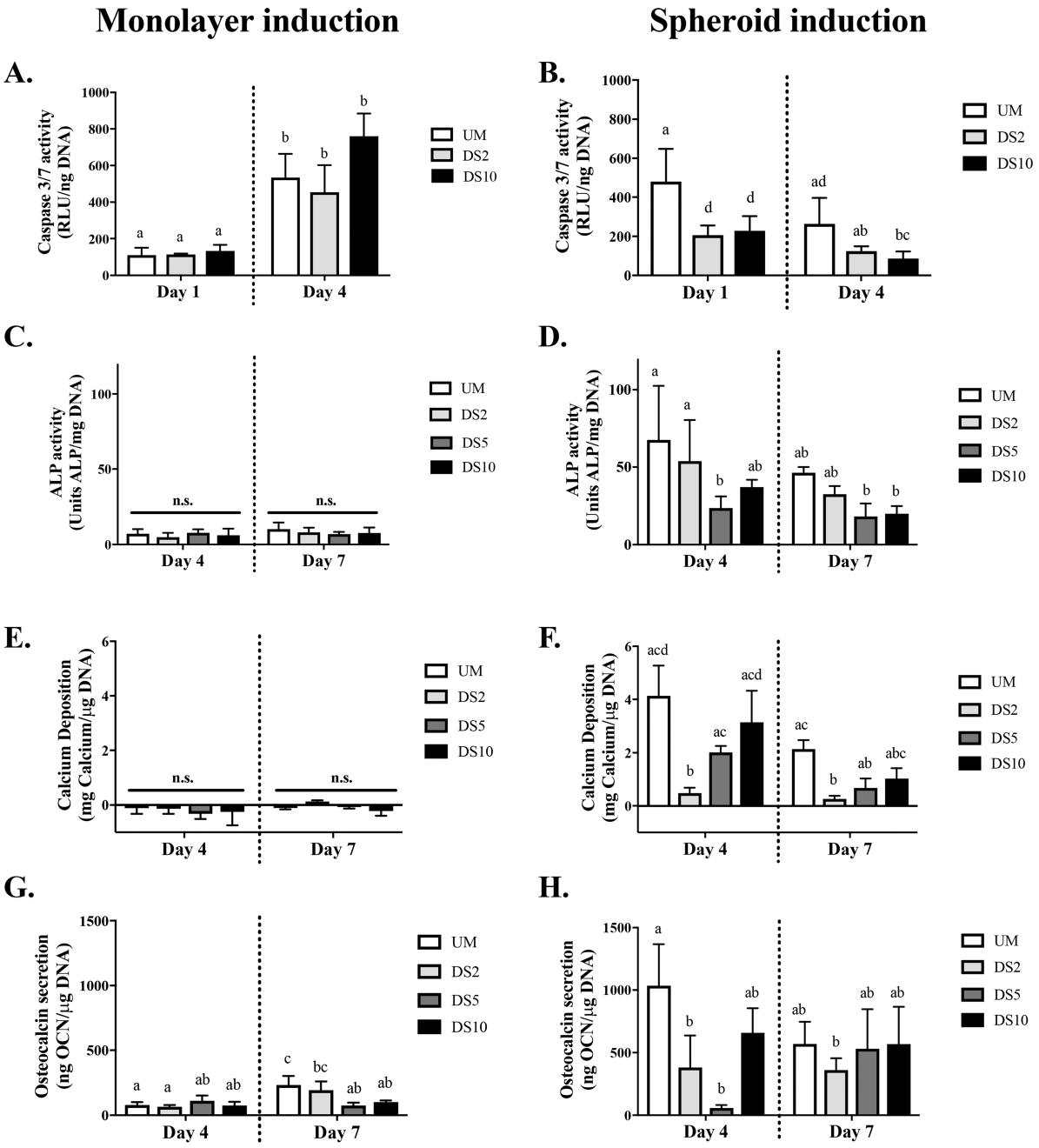

Figure 2.

RGD ligand density and osteoinduction of MSCs as spheroids improves cell viability and sustains osteoblastic markers. MSCs were osteoinduced under monolayer (A, C, E, G) or spheroid (B, D, F, H) culture. (A, B) Caspase 3/7 activity, (C, D) ALP activity, (E, F) calcium deposition, and (G, H) osteocalcin secretion. $n = 4$. Different letters indicate statistical significance; n.s. = not significant.

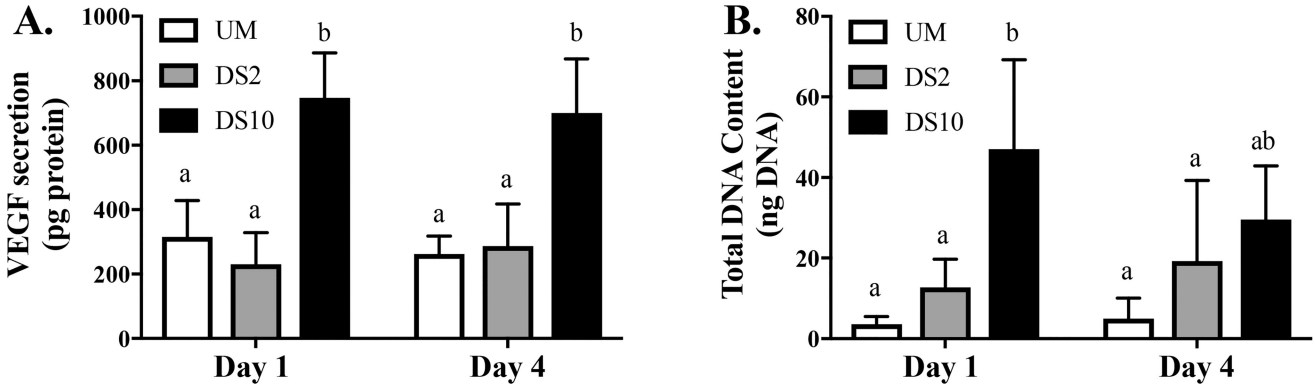

Figure 3.

Ligand density influences VEGF secretion by osteoinduced MSC spheroids. (A) Total VEGF secretion and (B) total DNA content; $n = 6$. Different letters indicate statistical significance.

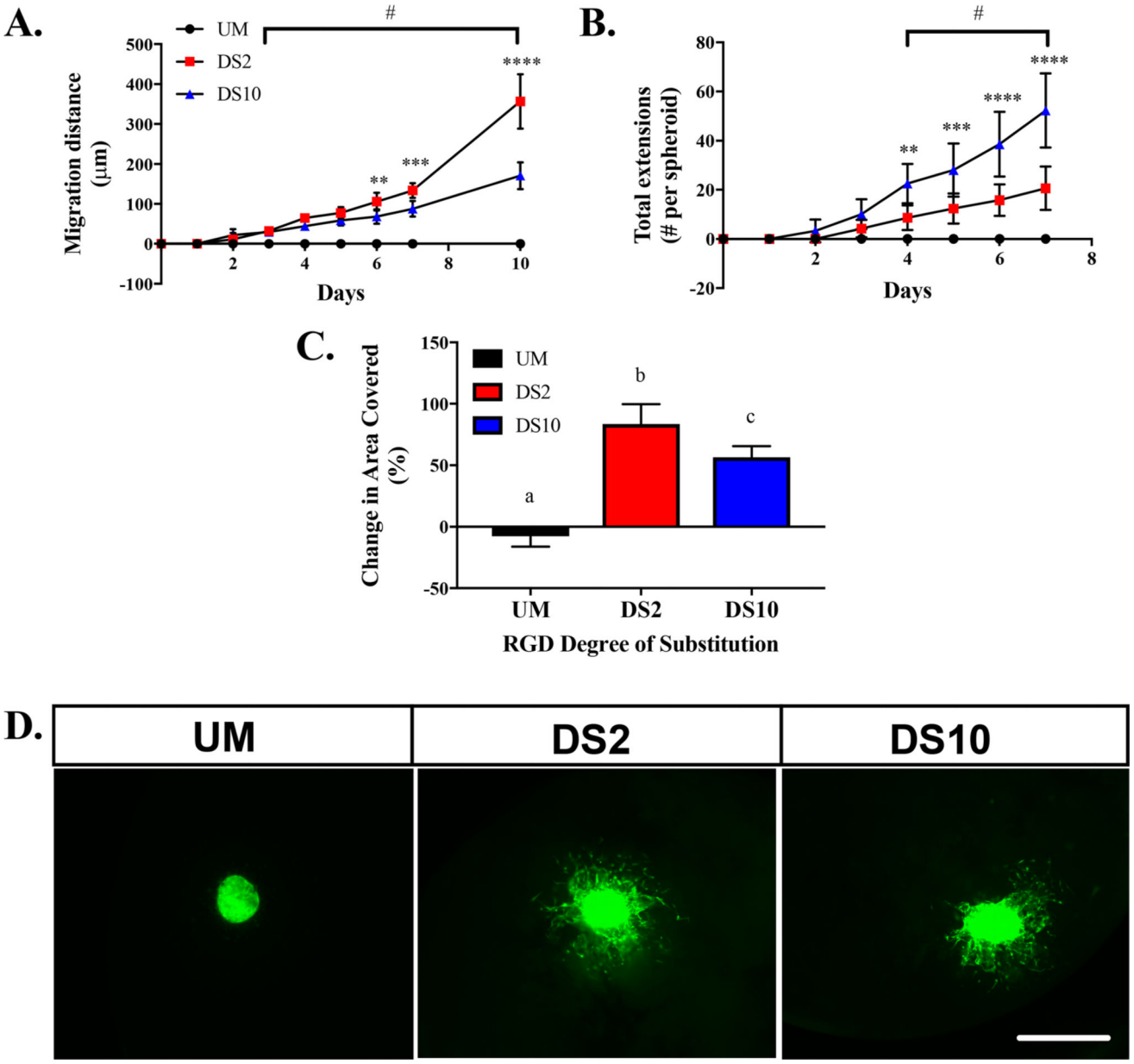

Figure 4.

RGD ligand density regulates osteoinduced spheroid migration kinetics. (A) MSC migration distance from spheroid over 10 days, (B) extension number over 7 days, and (C) spheroid change in area over 7 days; $n = 4$. *$p < 0.05$, **$p < 0.01$, ***$p < 0.001$, ****$p < 0.0001$ between DS2 and DS10. #$p < 0.05$ versus unmodified. (D) Representative fluorescent images of spheroids in unmodified, DS2, and DS10 alginate gels at Day 10. 4× magnification, scale bar = 500 μm.

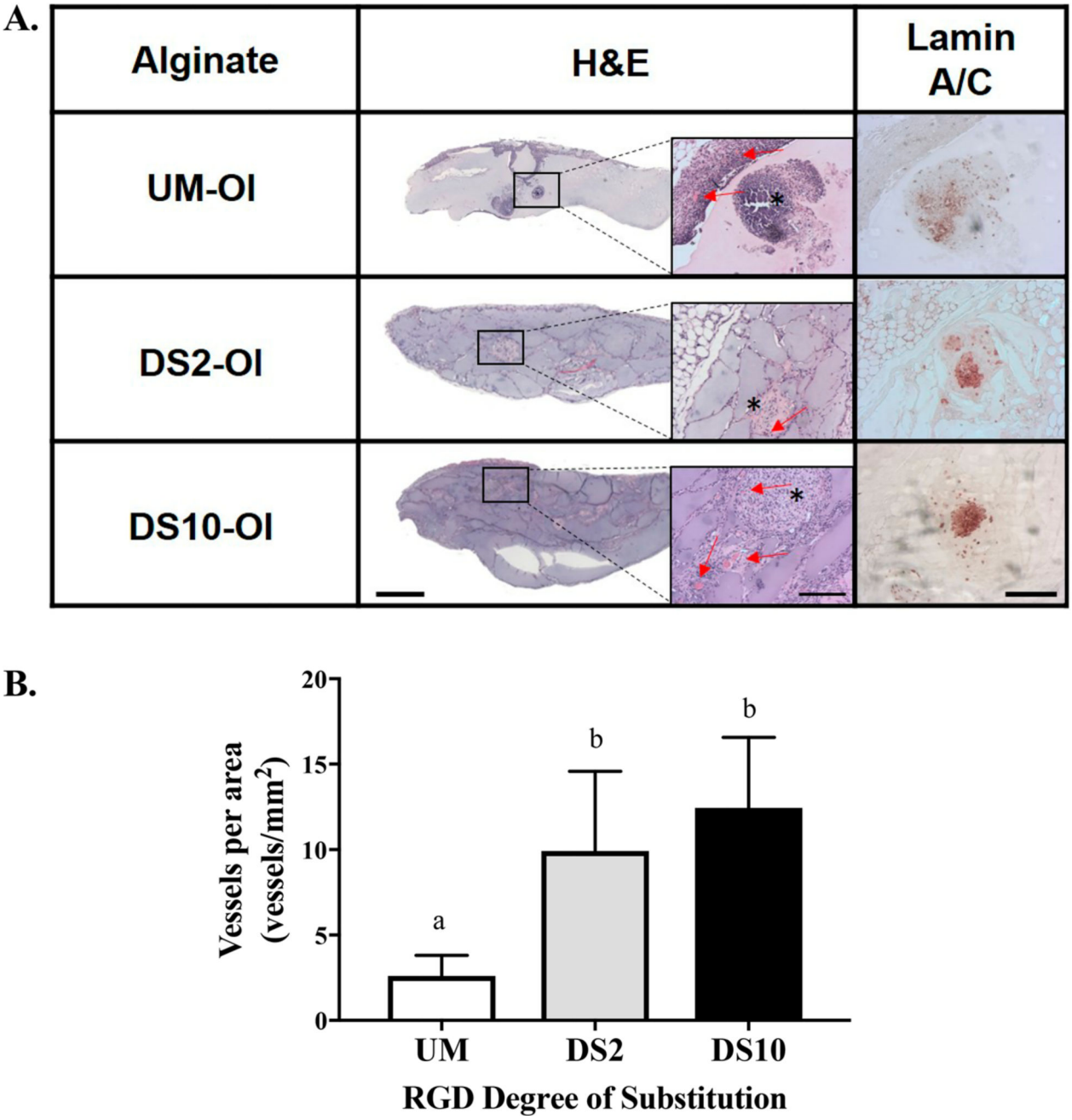

Figure 5.

RGD-modified alginate promotes neovessel formation and MSC persistence at 2 weeks. (A) Representative H&E staining of explants; scale bar = 1.0 mm. Insets represent images at 10× magnification; red arrows denote blood vessels, asterisks indicate spheroid; scale bar = 200 μm. Immunohistochemistry for lamin A/C; scale bar = 200 μm, 10× magnification. (B) Quantification of blood vessel density; $n = 5$ per group. Different letters indicate statistical significance.

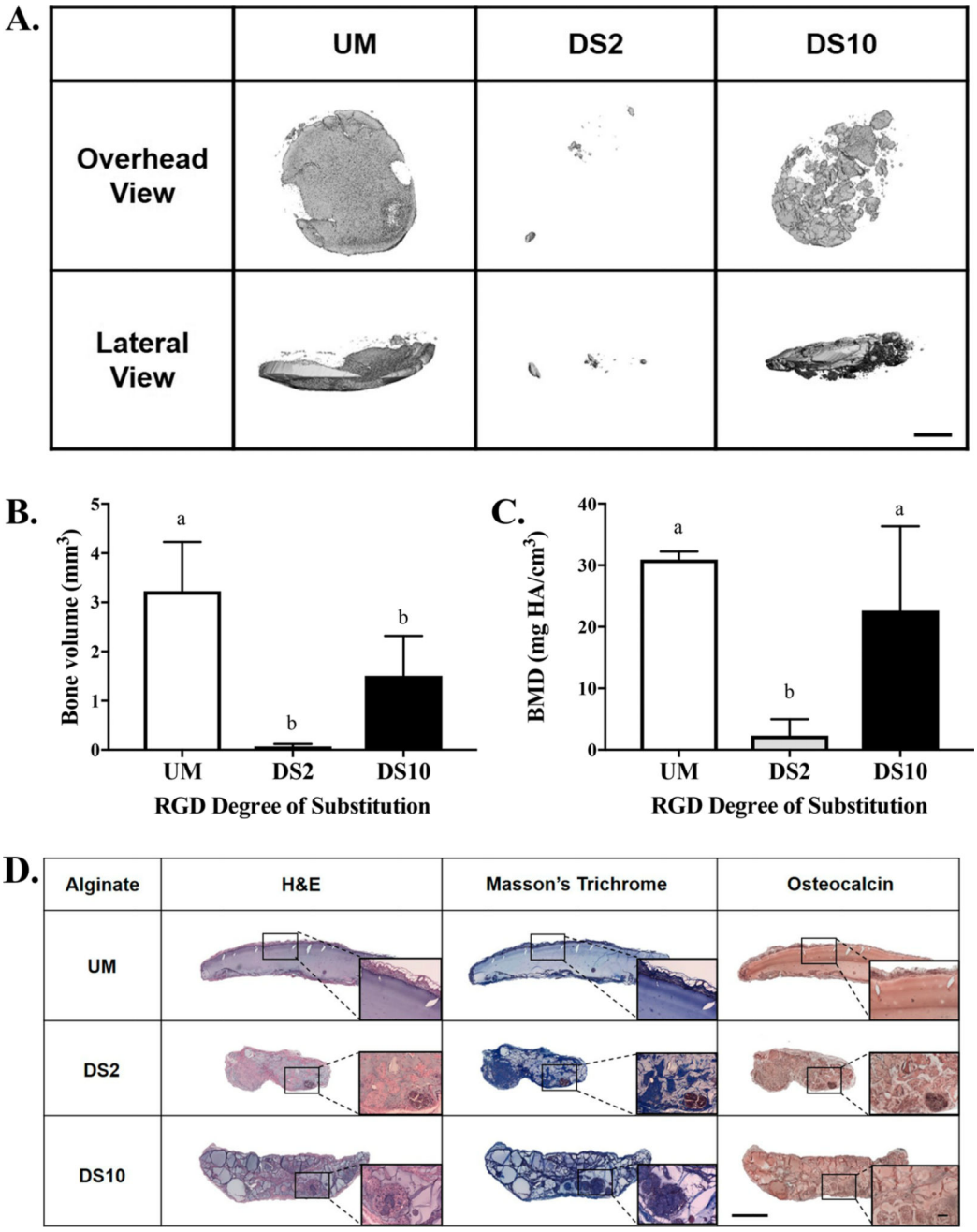

Figure 6.

Bone formation is increased by osteoinduced spheroids in alginates with increasing RGD density. (A) Representative microCT images of explants at 6 weeks. (B) Bone volume and (C) bone mineral density (BMD) determined from microCT scans; $n = 6$. Different letters indicate statistical significance. Scale bar = 1.0 mm. (D) Representative images of H&E, Masson's trichrome, and immunohistochemical stains for osteocalcin on 6 week explants. Scale bar = 1.0 mm. Insets taken at 10× magnification; scale bar = 200 μm.